

Kinetic effects in antiferromagnetic conductors with spin density waves

L. P. Gor'kov and A. V. Sokol

L. D. Landau Institute of Theoretical Physics, USSR Academy of Sciences

(Submitted 3 February 1987)

Zh. Eksp. Teor. Fiz. **93**, 2219–2231 (December 1987)

We investigate kinetic effects in metallic antiferromagnets with incommensurate spin density waves, in particular the conductivities of these systems. We show that the presence of a helicoidal spin density wave gives rise to a kinetic magnetoelectric effect. We show that the Froehlich conductivity mechanism can operate in these systems; this mechanism should manifest itself by "erasure" of the resistance maximum below the Néel point when the resistance is measured in sufficiently high fields. We discuss the possibility of observing these effects in a number of rare-earth antiferromagnets.

1. INTRODUCTION

The magnetoelectric effect, which consists of the appearance of a magnetic moment proportional to an applied electric field, is well-known in antiferromagnetic insulators.¹ Thus, in Ref. 2 it was pointed out that among the full crystal symmetry groups there are certain magnetic groups which do not possess space and time inversion symmetry among their elements. However, the authors of Ref. 3 noted that a magnetoelectric effect of kinetic origin could exist in nonmagnetic materials; in particular, these authors studied the case of conducting media which possess stereoisomerism. In this paper we will touch on some similar problems.

To be more specific, in what follows we will discuss a number of kinetic phenomena which are characteristic of conductors in which an incommensurate antiferromagnetic state forms, in particular a state with a helicoidal spin density wave (SDW). A fairly large number of systems are known, principally rare-earth metals and their compounds, in which such states have reliably been identified by neutron diffraction (see, e.g., Refs. 4 and 5). The helicoidal structure occurs often at fairly low temperatures. Usually the appearance of an SDW in a metal is accompanied by a number of anomalies, particularly in their electronic properties. Thus, e.g., the transition to the SDW state in dysprosium,⁶ holmium,⁷ and europium⁸ is accompanied by a drop in conductivity which usually is connected with the formation of an energy gap over part of the Fermi surface when the SDW forms.

As we said, the distinctive feature of rare-earth magnets is incommensurateness of the magnetic structure vector \mathbf{Q} with the period of the paramagnetic phase. In Ref. 9 these magnetic structures are referred to as "accidental," so as to emphasize that the period of the structure is a consequence not of symmetry but of the details of the structure of the Fermi surface, and is determined by the characteristics of the RKKY interaction. In particular, one widely accepted point of view is that the origin of the incommensurate structure is connected with flattened portions of the Fermi surface: just as for a one-dimensional problem, these portions lead either to instability of the electronic spectrum through their mutual overlap or to Kohn singularity in the RKKY interaction (see, e.g., Refs. 4, 5). The dependence of the vector \mathbf{Q} on temperature can be qualitatively understood if there are relatively close parts of the Fermi surface which satisfy overlap conditions ("nesting").

In addition to the SDW state which is "classical" for rare-earth magnetic systems, SDW states have been observed in a number of organic conductors and superconductors (see, e.g., the reviews Refs. 10, 11). In these quasi-one-dimensional compounds (the so-called Bechgard salts), the SDW state probably corresponds to a sinusoidal structure, because the antiferromagnetic vector formally appears commensurate (1:2) in relation to the period of the underlying lattice. It is possible, however, that the effects of commensurateness in such compounds might turn out to be rather weak. Neutron diffraction studies of the antiferromagnetic phase in these materials have not yet been carried out.

Experiments which study one-dimensional compounds suggest that a number of nontrivial phenomena can be connected with the appearance of incommensurate superstructures, including the magnetic ones, which go unnoticed in studies of the magnetism of conduction electrons in more classical systems. These phenomena also constitute the objects of study of this paper; specifically, we will discuss the "Froehlich conductivity" (i.e., a contribution to the conductivity due to motion of the incommensurate spin wave or charge density wave¹²), and the magnetoelectric effect alluded to above.

We will begin the study of Froehlich conductivity and the magnetoelectric effect by using terminology from the model usually employed to describe the properties of quasi-one-dimensional conductors, since incommensurateness has its most striking consequences—especially with regard to these effects—in these systems. Afterwards we will discuss those changes in the approach to the problem—and in estimates of various quantities—which must be made in order to treat more three-dimensional systems, e.g., SDWs in rare-earth antiferromagnets.

In Sec. 2 we describe an SDW model which in essence goes back to the original idea of Overhauser,¹³ and we discuss the equilibrium properties of this SDW state. In Sec. 3 we investigate the distinctive features of the conductivity which appear when the system enters the SDW state, and how this case differs from the analogous problem in the case of charge density waves (CDW). As we will see, it is possible for the properties of sinusoidal and helicoidal spin density waves to differ qualitatively at low temperatures. In Sec. 4 we present our results for the kinetic magnetoelectric effect. Finally, in Sec. 5 we will discuss estimates of the magnitude of these phenomena for three-dimensional conducting mag-

netic compounds; in the Conclusion we discuss the possibility of studying them experimentally.

2. MODEL

As we said above, we begin with a model in which the electronic state is characterized by a Fermi surface consisting of two open portions (see Fig. 1); its two sheets possess the overlap property ("nesting"):

$$\xi(\mathbf{p}) = -\xi(\mathbf{p} + \mathbf{Q}) \quad (1)$$

(degeneracy of the form (1) defines the so-called Keldysh-Kopaev model¹⁴). In this model, the generalized susceptibility $\chi(\mathbf{Q}, \omega, T)$ is logarithmically divergent; the usual Stoner criterion for a transition to the new phase

$$\chi = \frac{\chi_0}{1 - I(\mathbf{Q})\chi_0} \quad (2)$$

is that the denominator in (2) vanish. We will not discuss the mechanism by which the interaction $i(\mathbf{Q})$ in (2) gives rise to the antiferromagnetic phase itself, but rather will take this as an experimental fact. Thus, in the Bechgaard compounds we mentioned earlier, the ground state at low temperatures does in fact correspond to antiferromagnetic order; this has been proved by a multitude of experiments. We will investigate a hypothetical case where the spacing between the two parts of the Fermi surface shown in Fig. 1 is arbitrary, and consequently the wave turns out to be incommensurate.

Even when the wave is incommensurate, determining whether it is helicoidal or sinusoidal is a separate problem. In rare-earth compounds this problem has an explicit solution connected with the form of the RKKY interaction. We will investigate both the helicoidal and sinusoidal cases, although many unusual properties are connected with the helicoidal structure alone.

The order parameter corresponding to pairing of electrons and holes belonging to different spin branches on the two portions of the Fermi surface of Fig. 1 has the form

$$\hat{\Delta}_{RL} = (\hat{\mathbf{a}}\mathbf{d}) \exp(i\mathbf{Q}\mathbf{r}), \quad (3)$$

the spin-orbit interaction is assumed to be weak (we will neglect the dependence of $\hat{\Delta}$ on the position of points of the Fermi surface for simplicity). The sinusoidal wave corresponds to a real vector \mathbf{d} . For a helicoidal structure,

$$\mathbf{d}^2 = 0, \quad (3')$$

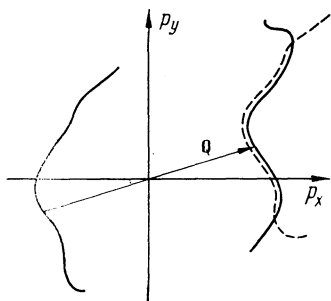


FIG. 1. Schematic form of overlapping portions of the Fermi surface.

i.e., \mathbf{d} is a complex vector $\mathbf{d}_1 + i\mathbf{d}_2$, with $\mathbf{d}_1 \perp \mathbf{d}_2$ and $|\mathbf{d}_1| = |\mathbf{d}_2|$.

Below T_N , the degeneracy of the spectrum is lifted because of the order parameter (3). The system of Green's functions satisfies the equations

$$(iz - \xi)\hat{G}_{RR} - \hat{\Delta}_{RL}\hat{G}_{LR} = \hat{1}, \quad (iz + \xi)\hat{G}_{LR} - \hat{\Delta}_{LR}\hat{G}_{RR} = \hat{0}. \quad (4)$$

We recall that (3) is proportional to the nondiagonal average $\hat{\Delta}_{RL} \propto \langle \psi_{R\alpha} \psi_{L\beta}^+ \rangle$; it is easy to verify that $\hat{\Delta}_{RL}^+ = \Delta_{RL}$.

The determinant of the left side of the system (4) determines a new energy excitation spectrum. If the wave is sinusoidal, then the spectrum always has a gap:

$$\varepsilon(\mathbf{p}) = \pm(\xi^2 + |\Delta|^2)^{1/2}. \quad (5)$$

If the structure is helicoidal, then, as was first noted in Ref. 13, the two-branched spectrum, corresponding to two spin directions, has a different form for right- and left-handed polarizations:

$$\hat{\varepsilon}_R^2(\mathbf{p}) = \xi^2 + |\mathbf{d}|^2(1 + \delta_z), \quad (5')$$

$$\hat{\varepsilon}_L^2(\mathbf{p}) = \xi^2 + |\mathbf{d}|^2(1 - \delta_z).$$

Here, the spin directions are relative to the vector

$$\mathbf{n} = i[\mathbf{d}\mathbf{d}^*] / |\mathbf{d}|^2. \quad (6)$$

Taking these definitions into account, the solutions to the system (4) corresponding to a helicoidal SDW in a pure metal ($\tau_{\text{imp}} \rightarrow \infty$) have the form

$$\hat{G}_{RR} = \frac{1 - \delta_z}{2} G_R^0 + \frac{1 + \delta_z}{2} G_R, \quad \hat{G}_{LR} = \hat{\Delta}_{LR} F, \quad (7)$$

where

$$G_R^0 = (iz - \xi)^{-1}, \quad G_R = -\frac{iz + \xi}{z^2 + \xi^2 + 2|\mathbf{d}|^2},$$

$$F = -\frac{1}{z^2 + \xi^2 + 2|\mathbf{d}|^2}. \quad (8)$$

The value of the order parameter depends on temperature. The most general form of the self-consistency condition is

$$\hat{\Delta}_{LR} = -\hat{K}(\hat{\Delta})\hat{G}_{LR}(x, x), \quad (9)$$

where the kernel \hat{K} is written so as to emphasize the probable dependence of the interaction, corresponding to the appearance of the SDW, on the restructuring of the electronic spectrum. We will not use the explicit form of \hat{K} in what follows (the value of the order parameter will depend on the form of the kernel \hat{K} in the temperature interval below T_N).

For a sinusoidal wave, the thermodynamic functions behave in the usual way: the electronic specific heat decreases exponentially for $T \ll T_N$, and the susceptibility is anisotropic. In order to determine the susceptibility correctly, it is appropriate, as usual, to introduce terms involving the magnetic anisotropy energy, which fix the spin direction. Then in weak fields the susceptibility along the spin direction falls rapidly below T_N , while transverse to the field it retains the value of the normal phase. In sufficiently strong fields the so-called "spin-flop" transition occurs (see, e.g., Ref. 15).

In the case of helicoidal waves, the specific heat at low

temperatures passes over to a linear dependence with Sommerfeld constant twice as small as in the normal phase. The susceptibility equals that of the normal phase for fields along the vector \mathbf{n} . For fields perpendicular to \mathbf{n} , the susceptibility drops by a factor of two.

In subsequent sections it will be necessary to introduce a small quantity of impurities, so as to include a source of dissipation in the kinetic effects at low temperatures. The role of impurities in the case of a sinusoidal wave is rather trivial—at small impurity concentrations, their primary effect is to lower the transition temperature. There is a more interesting effect connected with impurities in a helicoidal wave—even arbitrarily small concentrations of nonmagnetic impurities “smear out” the gap between the branches of the spectrum (5'). We note that the predominance of the elastic scattering by impurities corresponds to the case $T \ll \Omega$, where Ω is the Debye temperature.

Let us dwell on this latter phenomenon in more detail. For simplicity we consider a model of defects in which no forward scattering occurs. This methodological simplification leads to the disappearance of diagrams of the sort shown in Fig. 2, corresponding to “dressing” of the order parameter. The results must obviously contain only the transport time τ_{imp} (in our model it is double the probability for backward scattering). Including the impurities, we obtain a system of equations for the Green's functions:

$$\begin{aligned} \left(iz - \xi - \frac{1}{4\pi\tau_{imp}} \hat{G}_{LL} \right) \hat{G}_{RR} - \hat{\Delta}_{RL} \hat{G}_{LR} &= \hat{1}, \\ \left(iz + \xi - \frac{1}{4\pi\tau_{imp}} \hat{G}_{RR} \right) \hat{G}_{LR} - \hat{\Delta}_{LR} \hat{G}_{RR} &= \hat{0}. \end{aligned} \quad (10)$$

Here,

$$\hat{G} = \int \hat{G} d\xi. \quad (11)$$

For studying kinetic phenomena we require the analytic continuation of the solutions of (10) to the real frequency axis, i.e., $iz \rightarrow z$. Throughout the remainder of this section the upper sign in the formulas (\pm) corresponds to retarded functions (r), while the lower sign denotes advanced (a) functions. It is easy to see that the resulting continuations will be

$$\begin{aligned} G_R^0 &= \left(z - \xi \pm \frac{i}{4\tau_{imp}} \frac{z \pm i/4\tau_{imp}}{[(z \pm i/4\tau_{imp})^2 - 2|\mathbf{d}|^2]^{1/2}} \right)^{-1}, \\ G_R &= \frac{z + \xi \pm i/4\tau_{imp}}{(z \pm i/4\tau_{imp})^2 - \xi^2 - 2|\mathbf{d}|^2}, \\ F &= \frac{1}{(z \pm i/4\tau_{imp})^2 - \xi^2 - 2|\mathbf{d}|^2}. \end{aligned} \quad (12)$$

From the expression for the causal function G_R on the real axis we obtain for the density of states in the “gap” portion of the spectrum



FIG. 2. Diagram corresponding to the correction to the order parameter due to impurities.

$$\begin{aligned} N(z) &= N_0 \operatorname{Re} \left\{ \left(z + \frac{i}{4\tau_{imp}} \operatorname{sgn} z \right) \right. \\ &\quad \left. \times \left[\left(z + \frac{i}{4\tau_{imp}} \operatorname{sgn} z \right)^2 - 2|\mathbf{d}|^2 \right]^{-1/2} \right\}. \end{aligned} \quad (13)$$

In other words, because of the impurities the density of states at the Fermi level becomes finite (not zero!):

$$N(0) = N_0 (1 + 32(|\mathbf{d}| \tau_{imp})^2)^{-1/2}. \quad (13')$$

For the sinusoidal-phase Green's function we have

$$\hat{G}_{RR} = -\frac{i\tilde{z} + \xi}{\tilde{z}^2 + \xi^2 + |\Delta|^2}, \quad \hat{G}_{LR} = -\frac{\hat{\Delta}_{LR}}{\tilde{z}^2 + \xi^2 + |\Delta|^2}, \quad (14)$$

\tilde{z} satisfies the equation

$$\tilde{z} = z \pm \frac{1}{4\tau_{imp}} \frac{\tilde{z}}{(\tilde{z}^2 + |\Delta|^2)^{1/2}},$$

which is well-known from the theory of superconductors with paramagnetic impurities.¹⁶

The gapless situation corresponds to the values $1/\tau_{imp} \sim |\Delta|$ near the critical concentration of defects $1/\tau_c$, above which formation of the SDW is suppressed.

3. CONDUCTIVITY OF THE ANTIFERROMAGNETIC PHASE

Let us first investigate the behavior of the conductivity in the vicinity of the Néel point T_N . In rare-earth metals and their compounds, $T_N \sim 100$ – 200 K, i.e., it is larger by an order of magnitude or comparable to the Debye temperature. Here, the basic mechanisms of electron relaxation in the paramagnetic phase are phonon and magnetic scattering. (The contribution of critical fluctuations near T_N , judging by the function $\rho(T)$ in the experiments of Refs. 6–8, is apparently small). Below the transition point, as long as $|\mathbf{d}| \ll T_N$ holds the effective electron relaxation time τ differs little from its value in the metallic phase. In this region the dominant role of collisions involving phonons also ensures rapid energy relaxation of electrons. As for the assumptions listed above, the conductivity calculations are found to be fully analogous to those in Ref. 17, in which the same question was addressed for structural transitions in transition-metal trichalcogenides. We first discuss expressions for a fixed spin-density wave (the electric field satisfies $E < E_c$, where E_c is the field above which the wave is disrupted by pinning impurities or by commensurateness effects).

The expressions for the corrections to the conductivity in the sinusoidal-wave or helicoidal-wave phase differ only by the different number of gaps between the branches of their electronic spectra. Thus, for the helicoidal phase we have in our model (1):

$$\sigma(T) = \sigma_0 \left(1 - \frac{\pi |\mathbf{d}|^2 \tau}{2T_N (1 + 8(|\mathbf{d}| \tau)^2)^{1/2}} \right). \quad (15)$$

For the sinusoidal phase we have

$$\sigma(T) = \sigma_0 \left(1 - \frac{\pi |\Delta|^2 \tau}{2T_N (1 + 4(|\Delta| \tau)^2)^{1/2}} \right). \quad (15')$$

For $|\mathbf{d}| \tau \gg 1$ and $|\mathbf{d}| \ll T_N$, the decrease in conductivity corresponds to a fraction of electrons $\sim |\mathbf{d}|/T_N$ which pass “under the gap”. In the region $|\mathbf{d}| \tau \ll 1$ expression (15) has a precise meaning only when the model (1) is used and where the mean-field approximation is valid; for more realistic systems it retains only a qualitative character.

It is also interesting to investigate the conductivity in

the region of rather low temperatures, i.e., in the region of "residual resistivity," where the scattering processes which occur are due to defects. It is in this temperature region that the structural difference in the electronic spectrum between the sinusoidal and helicoidal phases alluded to in the previous section is most evident. In the sinusoidal phase there are no gapless branches, and for a model with a Fermi surface having aligned sheets the conductivity behavior (for pinning of the wave) corresponds to that of metal-insulator transitions. In the helicoidal phase, it is possible at low temperatures to have "metallization" of the conductivity, i.e., the conductivity goes up as the temperature decreases and exceeds the value that it would have in the paramagnetic state, in contrast to the fall in conductivity one would expect intuitively due to the decrease (by a factor of two) in the effective number of carriers. The origin of this behavior is, however, quite transparent physically. From the form of the spectrum (5') it follows that the "gap" and "gapless" branches are found on different regions of the original Fermi surface for the same spin. If we neglect scattering mechanisms which mix different spin channels, as the order parameter for the hexagonal phase forms and proceeds to grow, the mean free path of the gapless portion of the excitations increases because backward scattering for these portions is weakened by the small density of states in the gap branch on the opposite side of the Fermi surface. Finally, in this mechanism the electron energy is essentially conserved in the scattering event. Therefore, it is possible for the conductivity to increase due to this mechanism if inelastic phonon processes are infrequent. Near the Néel point this effect would be possible only in the case where the Néel temperature itself is small, i.e., $T_N \ll \Omega$. Unfortunately, we know of no example of a real antiferromagnetic transition to the helicoidal phase at low temperatures. The mechanism we have described for conductivity increase in the antiferromagnetic phase is not unique; for example, as the temperature decreases there is a "freezeout" of the scattering by fluctuations in the ion spins. Furthermore, in real systems the antiferromagnetic structure does not affect the entire Fermi surface; the remaining part should give an ordinary metallic contribution to the conductivity, which leads to a residual resistivity only at very low temperatures. The presence of these portions of the Fermi surface also weakens the effect in question itself, since it is the total "transport" relaxation time which is reflected in the conductivity, which now is not determined by strictly backward-scattering processes. We will return to this in Sec. 5.

Turning to the quasi-one-dimensional model, we will assume that $T_N \tau_{\text{imp}} \gg 1$ (i.e., the sample is very pure). The details of the calculation for impurity scattering are presented in the Appendix. We find for the low-temperature conductivity

$$\sigma = \sigma_{\text{res}} 4/2 |\mathbf{d}| \tau_{\text{imp}}, \quad (16)$$

where σ_{res} is the residual resistivity of the normal metal while τ_{imp} is the transport-impurity-scattering time.

Thus, in quasi-one-dimensional conductors with helicoidal structure the conductivity behaves as follows as the temperature changes: for $T_N \gtrsim \Omega$, then near T_N the conductivity $\sigma(T)$ falls; however, with a further decrease in temperature it begins to increase again, and near zero it becomes larger by a factor $\sim |\mathbf{d}| \tau_{\text{imp}}$ than it would be in the absence of

the magnetic structure. For $T_N \ll \Omega$ the conductivity

$$\sigma(T) = \sigma_0 \left(1 + \frac{\pi |\mathbf{d}|^2 \tau_{\text{imp}}}{4 T_N} \right) \quad (17)$$

(for $|\mathbf{d}| \ll 1/\tau_{\text{imp}} \ll T_N$) increases directly below T_N .

Up to now we have assumed that the spin density wave is immovable ($E < E_c$). Much remains unclear concerning the problem of pinning of SDW by impurities. The interaction of the SDW with impurities may have a local character (spin-orbit interaction), or is perhaps connected with distortion in the density of states (an effect which is second-order in the SDW amplitude); finally, the SDE may be due to fluctuations in the impurity distribution, since the local SDW energy and its Néel point T_N depend on the impurity concentration. In all these cases the pinning is expected to be weaker or of the same order of magnitude as for charge density waves. Just as for charge density waves (let us say, in the transition-metal trichalcogenides), it is also reasonable for us to expect effects in the incommensurate SDW phase which are analogous to the phenomenon of so-called Froehlich conductivity—motion of the wave as a whole under the action of a strong electric field ($E > E_c$). Actually, the contribution to the current from motion of the wave in the model under investigation contains a combination $(\hat{\Delta}_{RL} \hat{\Delta}_{LR} + \hat{\Delta}_{LR} \hat{\Delta}_{RL}) \varphi$ which is proportional to $\delta_{\alpha\beta}$ both for CDWs and SDWs. Therefore the motion of an SDW is connected with charge transfer¹² and not spin, as one might suppose. The phenomena ought to be manifest in the I - V characteristics first of all as a nonlinearity in the region around the threshold field E_c which separates the conductivity regimes corresponding to fixed and moving waves.

The motion of an SDW as a whole corresponds to variation of its phase according to the rule $\varphi = \mathbf{u} \cdot \mathbf{Q}$, where \mathbf{u} is the drift velocity of the wave in the presence of electric field. From a symmetry point of view there is very little difference in the definition of \mathbf{u} between sinusoidal and helicoidal waves. In the first case, φ is simply the phase of the incommensurate order parameter (3), while in the second case there is an additional symmetry of the order parameter (3), since multiplication of (3) by the factor $\exp(i\varphi)$ can be compensated by rotation of the \mathbf{d}_1 and \mathbf{d}_2 in the vector $\mathbf{d} = \mathbf{d}_1 + i\mathbf{d}_2$ by an angle $\zeta = -\varphi$ around the axis \mathbf{n} (the helical rotation is equivalent to its progressive motion). Therefore the drift velocity of the helicoidal wave is determined by the relation $\mathbf{Q}\mathbf{u} = \dot{\varphi} + \dot{\zeta}$.

Omitting the details of the calculation, which again are fully analogous to the calculations of Ref. 17, we state the basic result: near T_N ($|\Delta_{RL}| \ll T_N$) the motion of the SDW in a strong electric field exactly balances the growth in resistivity (15) and (15') due to the behavior of the gaps in the electronic spectrum. After this cancellation, an estimate of the conductivity in the neighborhood of T_N when the wave moves gives in both cases

$$(\sigma - \sigma_0)/\sigma_0 \sim |\Delta_{RL}|^2 / T_N^2 \ll 1. \quad (18)$$

Observation of the cancellation (18) of the anomalous resistivity (15), (15') in a strong electric field would constitute a strong argument in favor of the correctness of our understanding of the phenomenon (the electric field should still be small on the scale of the electronic spectrum. The threshold fields in the trichalcogenides (NbSe₃ and TaSe₃ lie in the interval from 10 to 0.1 mV/cm).

4. THE MAGNETOELECTRIC EFFECT

As we have already mentioned,¹⁸ in the helicoidal antiferromagnetic phase a dissipative current flowing in the conductor gives rise to magnetization of the spins. For an arbitrary crystal symmetry, the connection between magnetization and electric field is given by the relation

$$M_i = \alpha_{ik} E_k, \quad (19)$$

where α_{ik} is a magnetoelectric pseudotensor. From the Onsager principle (see Ref. 3) it follows that a magnetoelectric effect of dissipative origin must also be accompanied by the conjugate effect

$$j_i = -(\alpha_{ik} + \alpha_{ki}) \dot{B}_k. \quad (20)$$

We repeat that the tensor α_{ik} differs from zero only in the helicoidal SDW phase, in which inversion is not a symmetry element of the system. Then

$$\alpha_{ik} = \alpha n_i m_k, \quad (21)$$

where the unit vector n is directed along the helical axis (in the exchange approximation this axis is not fixed), while the unit vector m is normal to the Fermi surface.

Within the model we have chosen to describe the helicoidal SDW, the appearance of magnetization when current flows along Q has an especially simple physical interpretation at low temperatures. Actually, according to (5') the branches of the spectrum corresponding to a given direction of spin (along n) have a gapless (i.e., normal) character on one part of the Fermi surface, whereas on the other part excitation of an electron requires at least the gap energy. Therefore, at low temperatures the current is due to redistribution of the normal left-handed and right-handed excitations at the Fermi surface (relative to the direction of the vector Q) which have different directions of spin. As a result of this redistribution, magnetization arises which is proportional to the magnitude of the current.

It is clear from what we have said so far that calculation of the magnetoelectric tensor (21) is from a mathematical standpoint completely analogous to calculating the conductivity. The magnetic moment in the presence of a current is expressed through corrections to the Green's functions which are linear in the electric field:

$$M \propto -\mu_B n (\bar{G}_{RR\uparrow}^{(4)} + \bar{G}_{LL\uparrow}^{(4)} - \bar{G}_{RR\downarrow}^{(4)} - \bar{G}_{LL\downarrow}^{(4)}),$$

we will not discuss these computations (see the Appendix), but rather will simply state the results immediately.

For the magnetoelectric constant α near the Néel point (in what follows, e denotes the absolute value of the electron charge) we obtain

$$\alpha = -\mu_B e S \frac{(|d|\tau)^2}{(2\pi)^2 T_N (1 + 8(|d|\tau)^2)^{1/2}}. \quad (22)$$

Here, S is the area of one of the portions of the Fermi surface shown in Fig. 1, and $|d| \ll T_N$. It is assumed that $T_N \gtrsim \Omega$, i.e., that phonon processes are significant.

For a moving wave (i.e., an electric field which exceeds threshold), under the same assumptions

$$\alpha \sim \mu_B e S \frac{|d|^2 \tau}{T_N^2}. \quad (23)$$

According to (23), as the wave becomes entrained the magnitude of the magnetoelectric effect falls sharply, as do the various anomalies in the conductivity, and may even change sign.

At low temperatures the relaxation time τ_{imp} is due to impurity collisions. For $T \ll T_N$ (a stationary wave) we obtain for the value of α

$$\alpha = -\mu_B e S \frac{2\sqrt{2}|d|\tau_{imp}^2}{\pi^3} \quad (24)$$

The study of effects related to SDW motion in this region is greatly complicated by variations in the mean free path, which will be discussed in Sec. 3. In view of the obviously model-dependent nature of the spectrum (1), we will not discuss this question here.

To conclude the section, we present an expression for α when $T_N \ll \Omega$ and elastic scattering plays a dominant role even near the Néel point:

$$\alpha = -\mu_B e S \frac{1}{16\pi^2 T_N} \quad (25)$$

(for a stationary wave). Equation (25) implies that the magnetoelectric effect appears discontinuously; however, this is because up to now we have not taken into account scattering processes which "entangle" the spin channels. Introducing a spin-orbit scattering with characteristic time τ_s , we obtain in place of (25)

$$\alpha = -\mu_B e S \frac{1}{16\pi^2 T_N} \left(\frac{|d|^2}{|d|^2 + 2(\tau_{imp}\tau_s)^{-1}} \right). \quad (25')$$

5. THE EFFECT OF A THREE-DIMENSIONAL FERMI SURFACE

In our specific calculations so far we have used a model in which the Fermi surface has two fully-overlapping sheets. This model is doubtless adequate in materials such as the quasi-one-dimensional conductors; in fact, an antiferromagnetic phase is actually observed at sufficiently low temperatures in the compounds $(TMTSF)_2X$, which are in fact one-dimensional. We have already noted earlier that the structural formula for these compounds formally corresponds to the presence of a commensurate SDW, due to the alternation of molecules in the TMTSF stack. Although it is not yet fully clear what the role of this alternation is—it is quite small—it has been established that it is connected with pinning of the SDW, and so the threshold fields are likely to be rather high, although this question has not been investigated.

In the rare-earth types of magnets there is a greater richness of incommensurate structures, in which—according to, e.g., Refs. 6–8—the kinetic properties of conduction electrons are notably affected by the antiferromagnetic transition. In the physical picture of Refs. 4, 5 the magnetic order is related to the presence of flattened (i.e., overlapping) portions on the Fermi surface; with this in mind, we will estimate how sensitive the effects mentioned above are to the fact that these portions make up only a fraction S_1/S from the area of an otherwise three-dimensional Fermi surface. Let us recall that we always have $T_N \ll E_F$.

We begin with the case where there are no such portions in general. Then according to Ref. 9, the incommensurate structure vectors Q coincide with the extremal diameters of the Fermi surface. We assert that for an isotropic Fermi sur-

face of the sort shown in Fig. 3, the order parameter with vector \mathbf{Q} couples parts of the surface near its poles. Let us again write this coupling in the form of equations for the Green's functions:

$$\begin{aligned} [iz - \varepsilon(\mathbf{p})] \hat{G}(z, \mathbf{p}) - \hat{\Delta}_{-Q} \hat{G}_Q(z, \mathbf{p}) - \hat{\Delta}_Q \hat{G}_{-Q}(z, \mathbf{p}) &= \hat{1}, \\ [iz - \varepsilon(\mathbf{p} - \mathbf{Q})] \hat{G}_Q(z, \mathbf{p}) - \hat{\Delta}_Q \hat{G}(z, \mathbf{p}) &= \hat{0}, \\ [iz - \varepsilon(\mathbf{p} + \mathbf{Q})] \hat{G}_{-Q}(z, \mathbf{p}) - \hat{\Delta}_{-Q} \hat{G}(z, \mathbf{p}) &= \hat{0}. \end{aligned} \quad (26)$$

As before

$$\hat{\Delta}_Q^+ = \hat{\Delta}_{-Q}. \quad (27)$$

It is obvious that the solution to (26) for the function $\hat{G}(z, \mathbf{p})$ near the poles differs from (7) and (8) only by the replacement

$$iz \rightarrow iz + 2t(\mathbf{p}_\perp), \quad (28),$$

where

$$\xi = v_F(\mathbf{p} - \mathbf{p}_F), \quad 2t(\mathbf{p}_\perp) = \frac{1}{2}[\varepsilon(\mathbf{p}) + \varepsilon(\mathbf{p} - \mathbf{Q})].$$

The "nondiagonal" functions $\hat{G}_{\pm Q}$ decrease rapidly as we move away from the poles: $\hat{G}_{\pm Q} \sim \hat{\Delta}/t^2(\mathbf{p}_\perp)$. For further estimates, let us assume isotropic impurity scattering:

$$\tau_{imp}^{-1} \propto \langle \overline{G(0, \mathbf{p})} \rangle \quad (29)$$

(The angle brackets denote integration over the entire Fermi surface.) Analogously, the conductivity σ_{ik} is determined by analytic continuation of the quantity

$$\sigma_{ik}(\omega) \propto \sum \langle v_{Fi} v_{Fk} \overline{G(iz, \mathbf{p}) G(iz - \omega, \mathbf{p})} \rangle. \quad (30)$$

According to (28), in the isotropic case contributions to anomalies in the physical quantities come from electrons with $p_\perp \sim p_F (\Delta/E_F)^{1/2}$. Near T_N , the fraction of electrons which pass under the gap and do not take part in the conductivity is $\Delta^2/T_N E_F$. Consequently, for an estimate of the rise in resistivity near T_N we have in place of (15)

$$(\sigma - \sigma_0)/\sigma_0 \sim -\Delta^2/T_N E_F. \quad (31)$$

Calculations analogous to those presented in Sec. 3 show that as the wave grows the anomalies (31) again are smoothed out by the Froehlich mechanism.

In the SDW model (Sec. 2) Δ is equal to T_N in order of magnitude ($\Delta/T_N \sim [(T_N - T)/T_N]^{1/2}$ near the Néel point). In the past it was assumed (see, e.g., Ref. 9) that the local moments of the f -shells are ordered by the Ruderman-

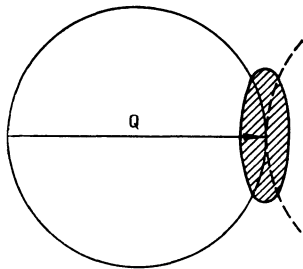


FIG. 3. Formation of a gap in an isotropic electronic spectrum when the magnetic structure vector equals an extremal diameter of the Fermi surface.

Kittel interaction: $T_N \sim J^2/E_F$, where J is the exchange interaction constant between the ion spins and conduction electrons:

$$\hat{H}_{ex} = J(\mathbf{S}\sigma).$$

Correspondingly, (31) is meaningful only near T_N ($\Delta(T) \ll T_N$). For $T \sim T_N$, we have $\Delta \sim J$ and the maximum conductivity decrease is determined by the fact that a small fraction

$$\Delta/E_F \sim J/E_F \sim (T_N/E_F)^{1/2} \ll 1$$

of the entire "isotropic" Fermi surface is closed off by the energy gap. The estimate we obtain in this way is apparently insufficient to explain the considerable rise in resistivity in a number of rare-earth metals below T_N ; this circumstance constitutes an important argument in favor of the presence of "flattened portions" of the Fermi surface.

For $T \lesssim T_N$, the role of such "planar" or overlapping portions (whose area we denote by S_1) in the kinetic effects discussed above is reduced to increasing the fraction of the Fermi surface which is closed off by an energy gap. We will define a portion as planar if the departure from overlap of the Fermi surfaces in (26) and (28) over the area S_1 is small, i.e., $t(\mathbf{p}_\perp) \lesssim \Delta$. However, the coupling of Δ with T , as we said earlier, depends on the mechanism of antiferromagnetism. In a Weissfield model, the antiferromagnetic order is induced by the RKKY interaction between local f -shells. The planar portions play a role here because a component of the RKKY interaction turns out to be large for the structure vector \mathbf{Q} corresponding to overlap of these portions. Below T_N , the RKKY interaction naturally depends on the reconstruction of the electronic spectrum; however, as we mentioned above, $\Delta \sim J \sim (T_N E_F)^{1/2}$ holds at sufficiently low temperatures. Another possibility worth mentioning which involves the planar portions is energetic instability of the spectrum (1), by virtue of which the electronic subsystem can itself initiate a transition to the antiferromagnetic phase for $T_N = T_{SDW} > J^2/E_F$. In this case, the portion is "planar" wherever $t(\mathbf{p}_\perp) \lesssim T_{SDW}$ holds while $\Delta \sim T_{SDW}$.

Returning to the results we obtained earlier, we see that the increased conductivity effect in a helicoidal wave, which was discussed in Sec. 3, will or will not take place depending on the specific scattering mechanisms, in particular on how large the fraction of backward scattering is in (29), i.e., in that part of the Fermi surface where a gap opens up for $T < T_N$.

Because of this, the magnetoelectric effect becomes smaller at low temperatures, and is determined only by the fraction of planar portions. In place of (27), we obtain the estimate

$$\alpha \sim -\mu_B e S_1 \tau_{imp} / 4\pi^3, \quad S_1 \ll S. \quad (24')$$

Analogously, a factor S_1/S appears in (15), (15') for the conductivity correction.

6. CONCLUSION

Independent of our choice of model, the results we have presented point to the presence of Froehlich conductivity mechanisms in incommensurate spin structures. The most

striking manifestation of these mechanisms would consist of the predicted leveling of the resistivity maximum below T_N at fairly low electric field intensities. In the usual descriptions of SDW pinning, the latter is unimportant either for fields above threshold or when the conductivity measurement is made in a VHF field. (In NbSe_3 this is the centimeter-to-millimeter band.)

Nevertheless, the planar portions apparently do play an important role in rare-earth antiferromagnets. The Fermi surface in these systems is probably quite complex, consisting of many sheets. Therefore, the function $\mathbf{Q}(T)$ does not contradict these assumptions (compare Ref. 9); however, any quantitative theoretical expressions would contain a number of indeterminate characteristics of the spectrum. As for the question of whether the mechanism for the transition to the antiferromagnetic phase is induced by energetic instability of this spectrum or whether it is better understood in terms of the usual Ruderman-Kittel interaction, this question is still open.^{4,5}

For the majority of such effects, only the reconstruction of the electronic spectrum itself due to the order parameter (27) is significant, independent of the mechanism of the magnetism. Observation of the magnetoelectric effect in a helicoidal antiferromagnetic structure would give direct information about this reconstruction. In all likelihood, the phenomenon is most convenient to observe in the form represented by (20), i.e., in measuring the potential difference induced in a single-domain sample by a variable magnetic field applied along the helical axis:

$$eE \sim \frac{\mu_B}{v_F} \frac{S_1}{S} \dot{H}.$$

Estimates for $H \sim 100$ e, $\omega \sim 1$ GHz would give $E \sim 10^{-6}$ to 10^{-7} V/cm.

The authors are deeply grateful to I. E. Dzyaloshinski, R. Z. Levitin, V. V. Tugushev, and G. M. Eliashberg for useful discussions and comments.

APPENDIX

Using the assumptions of Secs. 2, 3 concerning impurities, we have the following equation for the correction to the Green's function in the field on the Matsubara frequency axis (below we will write τ for τ_{imp} for brevity; $e = |e|$):

$$\begin{aligned} \hat{G}_{RR}^{(1)}(z_1, z_2) &= \hat{G}_{RR}(z_1) \left\{ \frac{e}{c} (vA) + \frac{1}{4\pi\tau} \hat{G}_{LL}^{(1)}(z_1, z_2) \right\} \hat{G}_{RR}(z_2) \\ &+ \hat{G}_{RL}(z_1) \left\{ -\frac{e}{c} (vA) + \frac{1}{4\pi\tau} \hat{G}_{RR}^{(1)}(z_1, z_2) \right\} \hat{G}_{RL}(z_2), \\ \hat{G}_{LL}^{(1)}(z_1, z_2) &= \hat{G}_{LL}(z_1) \left\{ -\frac{e}{c} (vA) + \frac{1}{4\pi\tau} \hat{G}_{RR}^{(1)}(z_1, z_2) \right\} \hat{G}_{LL}(z_2) \\ &+ \hat{G}_{LR}(z_1) \left\{ \frac{e}{c} (vA) + \frac{1}{4\pi\tau} \hat{G}_{LL}^{(1)}(z_1, z_2) \right\} \hat{G}_{RL}(z_2). \end{aligned} \quad (\text{A1})$$

Decomposing the function $\hat{G}^{(1)}$ for helicoidal waves into spin projections

$$\hat{G}^{(1)} = G_{\uparrow}^{(1)} \frac{1+\delta_z}{2} + G_{\downarrow}^{(1)} \frac{1-\delta_z}{2}, \quad (\text{A2})$$

we see that

$$\bar{G}_{RR\uparrow}^{(1)} = -\bar{G}_{LL\downarrow}^{(1)}, \quad \bar{G}_{RR\downarrow}^{(1)} = -\bar{G}_{LL\uparrow}^{(1)}. \quad (\text{A3})$$

The current contains the combination of occupation numbers $\sum_i v_i \text{Sp} \delta \hat{n}_i$:

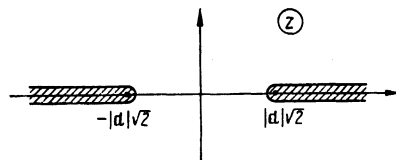


FIG. 4. Choice of analytic branches in the conductivity expressions (see Appendix).

$$\bar{G}_{RR\uparrow}^{(1)} + \bar{G}_{RR\downarrow}^{(1)} - \bar{G}_{LL\uparrow}^{(1)} - \bar{G}_{LL\downarrow}^{(1)}, \quad (\text{A4})$$

however, this must be computed on the real frequency axis. Analytic continuation of (A1), (A4) gives the equation¹⁹

$$\begin{aligned} T \sum_i G^{(1)}(z, z-\omega) &\rightarrow \int \frac{dz}{4\pi i} \left\{ \text{th} \frac{z-\omega}{2T} G^{(1)rr}(z, z-\omega) \right. \\ &- \text{th} \frac{z}{2T} G^{(1)aa}(z, z-\omega) \\ &\left. + \left(\text{th} \frac{z}{2T} - \text{th} \frac{z-\omega}{2T} \right) G^{(1)ra}(z, z-\omega) \right\}. \end{aligned} \quad (\text{A5})$$

The indices r and a denote retarded and advanced Green's functions, respectively. The contribution to the current is determined by the nonregular terms of the form

$$G^r(z) G^a(z-\omega) \frac{\omega}{2T \text{ch}^2(z/2T)}.$$

Calculating these latter, let us say, for the right-hand part of the Fermi surface gives

$$\begin{aligned} \bar{G}_{RR\uparrow}^{(1)ra}(z, z-\omega) &= \frac{e}{c} (vA) I_g^{ra} \left(1 - \frac{1}{4\pi\tau} I_n^{ra} \right) \left(1 - \frac{1}{16\pi^2\tau^2} I_n^{ra} I_g^{ra} \right)^{-1}, \\ \bar{G}_{RR\downarrow}^{(1)ra}(z, z-\omega) &= \frac{e}{c} (vA) I_n^{ra} \left(1 - \frac{1}{4\pi\tau} I_g^{ra} \right) \left(1 - \frac{1}{16\pi^2\tau^2} I_n^{ra} I_g^{ra} \right)^{-1} \end{aligned} \quad (\text{A6})$$

Here, in turn, we introduce the notation

$$\begin{aligned} I_n^{ra} &= \int d\xi G_R^{0r}(z) G_R^{0a}(z-\omega), \\ I_g^{ra} &= \int d\xi \{ G_R^r(z) G_R^a(z-\omega) - 2|d|^2 F^r(z) F^a(z-\omega) \}. \end{aligned} \quad (\text{A7})$$

Expression (A7) gives

$$\begin{aligned} I_n^{ra} &= 8\pi\tau \left[\frac{z+i/4\tau}{((z+i/4\tau)^2 - 2|d|^2)^{1/2}} \right. \\ &\quad \left. - \frac{z-\omega-i/4\tau}{((z-\omega-i/4\tau)^2 - 2|d|^2)^{1/2}} \right]^{-1}, \\ I_g^{ra} &= \frac{2\pi\tau}{z-\omega/2} \left[\frac{(z-\omega/2)(z+i/4\tau) - 2|d|^2}{[(z+i/4\tau)^2 - 2|d|^2]^{1/2}} \right. \\ &\quad \left. - \frac{(z-\omega/2)(z-\omega-i/4\tau) - 2|d|^2}{[(z-\omega-i/4\tau)^2 - 2|d|^2]^{1/2}} \right]. \end{aligned} \quad (\text{A8})$$

The square root in these expressions is chosen so that $\text{Im}(z^2 - 2|d|^2)^{1/2} > 0$ (the cut in the complex plane is shown in Fig. 4).

The integrals in (A5) and (A6)–(A8) are easily evaluated for $T \ll |d|$. In particular, for $T_N \tau \gg 1$ the variations in the occupation numbers in (A4) are

$$\delta n_{R\uparrow} = \delta n_{L\downarrow} \cong 0, \quad \delta n_{R\downarrow} = -\delta n_{L\uparrow} = -eSE\pi^{-3}\sqrt{2}|d|\tau^2,$$

from which follow (16) and (24). Near T_N (if $T_N \ll \Omega$) we have

$$\begin{aligned} \delta n_{R\uparrow} &= -\delta n_{L\downarrow}, & \delta n_{R\downarrow} &= -\delta n_{L\uparrow}, \\ \delta n_{R\uparrow} + \delta n_{R\downarrow} &= -\frac{2eS\tau E}{(2\pi)^3} \left[1 + \frac{\pi|d|^2\tau}{4T_N} \right], \\ \delta n_{R\uparrow} - \delta n_{R\downarrow} &= \frac{eSE}{32\pi^2 T_N}, & |d| &\ll 1/\tau \ll T_N. \end{aligned}$$

¹L. D. Landau and E. M. Lifshits, *Electrodynamics of Continuous Media*, Pergamon, Oxford (1960).

²I. E. Dzyaloshinski, Zh. Eksp. Teor. Fiz. **37**, 881 (1959) [Sov. Phys. JETP **10**, 628 (1960)].

³L. S. Levitov, Yu. V. Nazarov, and G. M. Eliashberg, Zh. Eksp. Teor. Fiz. **88**, 229 (1985) [Sov. Phys. JETP **61**, 133 (1985)].

⁴B. Coqblin, *The Electronic Structure of Rare-Earth Metals and Alloys: The Magnetic Rare-Earths* (Academic Press: New York, 1977).

⁵E. T. Kulatov, N. I. Kulikov, and V. V. Tugushev, Proc. IOFAN, Vol. 3, 122 (1986).

⁶P. H. Hall, S. Levgold, and F. S. Spedding, Phys. Rev. **117**, 971 (1960).

⁷D. L. Strandburg, S. Levgold, and F. S. Spedding, Phys. Rev. **127**, 2046 (1962).

⁸M. A. Curry, S. Levgold, and F. S. Spedding, Phys. Rev. **117**, 953 (1960).

⁹I. E. Dzyaloshinski, Zh. Eksp. Teor. Fiz. **47**, 336 (1964) [Sov. Phys. JETP **20**, 223 (1965)].

¹⁰D. Jerome and H. J. Schulz, Adv. Phys. **31**, 299 (1982).

¹¹L. P. Gor'kov, Usp. Fiz. Nauk **144**, 381 (1984) [Sov. Phys. Usp. **27**, 809 (1984)].

¹²P. A. Lee, T. M. Rice, and P. W. Anderson, Sol. State Commun. **14**, 703 (1974).

¹³A. W. Overhauser, Phys. Rev. Lett. **4**, 462 (1960); Phys. Rev. Lett. **4**, 514 (1960).

¹⁴L. V. Keldysh and Yu. V. Kopaev, Fiz. Tverd. Tela **6**, 2791 (1964) [Sov. Phys. Sol. State **6**, 2219 (1964)].

¹⁵A. V. Sokol, Zh. Eksp. Teor. Fiz. **92**, 756 (1987) [Sov. Phys. JETP **65**, 426 (1987)].

¹⁶A. A. Abrikosov and L. P. Gor'kov, Zh. Eksp. Teor. Fiz. **39**, 1781 (1960) [Sov. Phys. JETP **12**, 1241 (1961)].

¹⁷L. P. Gor'kov and E. N. Dolgov, Zh. Eksp. Teor. Fiz. **77**, 396 (1979) [Sov. Phys. JETP **50**, 203 (1979)].

¹⁸L. P. Gor'kov and A. V. Sokol, Pis'ma Zh. Eksp. Teor. Fiz. **45**, 239 (1987) [JETP Lett. **45**, 235 (1987)].

¹⁹L. P. Gor'kov and G. M. Eliashberg, Zh. Eksp. Teor. Fiz. **54**, 612 (1968) [Sov. Phys. JETP **27**, 328 (1968)].

Translated by Frank J. Crowne